An evaluation of soil hydraulic parameter uncertainty on the hydrologic performances of oil sands reclamation covers

Md. Shahabul Alam, S. Lee Barbour & Mingbin Huang
Department of Civil, Geological and Environmental Engineering – University of Saskatchewan, Saskatoon, SK, Canada

ABSTRACT
The performance of oil sands reclamation covers is evaluated through the simulation of long-term water balance using calibrated soil-vegetation-atmosphere-transfer models. Conventional practice is to develop a single set of calibrated properties based on few monitoring data sets. The ability to characterize spatial or temporal variability in the cover properties is therefore limited. This study utilizes inverse modelling (IM) to optimize the hydraulic properties for 12 prototype covers, replicated in triplicate, at Syncrude's Aurora mine site. IM was used to optimize the hydraulic parameters for three soil types (peat, sandy subsoil, and lean oil sand) for each monitoring site from 2013-2016. 155 optimized parameter values helped define parameter uncertainty for each soil. Calibrated models were used to evaluate variations in the maximum sustainable LAI and quantify uncertainty associated with long-term water balance based on calibrated parameters and LAI values.

RÉSUMÉ
La performance des couvertures de remise en état des sables pétrolifères est évaluée grâce à la simulation du bilan hydrique avec des modèles calibrés de transfert sol-végétation-atmosphère. La pratique conventionnelle est de développer un ensemble de propriétés calibrées basées sur quelques ensembles de données de contrôle. La capacité de caractériser la variabilité spatiale ou temporelle des propriétés des couvertures est donc limitée. Cette étude utilise la modélisation inverse pour optimiser les propriétés hydrauliques de 12 prototypes de couvertures, répétés en trois exemplaires, au site minier Aurora de Syncrude. Elle a optimisé les paramètres hydrauliques pour trois types de sols (tourbe, sous-sol sablonneux et sables légèrement pétrolifères) pour chaque site de contrôle de 2013 à 2016. 155 valeurs de paramètres optimisées ont aidé à définir l'incertitude des paramètres de chaque sol. Les modèles calibrés ont permis d'évaluer les variations d'ISF maximum durable et de quantifier l'incertitude associée au bilan hydrique à long terme basé sur les paramètres calibrés et les valeurs ISF.

1 INTRODUCTION

The two key measures of success for oil sands mine reclamation covers are the water balance components of actual transpiration (AT) and net percolation (NP). AT quantifies the ability of the cover to support re-vegetation, while NP quantifies the release of water to adjacent wetlands or surface water and is central to estimates of chemical flushing from the underlying mine waste.

Conventional practice has been to monitor covers for a short-term period (e.g. 5-10 years) and then calibrate SVAT models to simulate the water balance over the long-term (e.g. 60 years). Previous studies (Huang et al. 2011a,b,c, 2015a; Keshta et al. 2009, Price et al. 2010; Qualizza et al. 2004) have relied on data from a single monitoring station to calibrate the SVAT models and consequently, the ability to characterize the spatial or temporal variability in cover properties was limited.

Temporal variability in hydraulic conductivity (Ks) was measured in reclamation covers over saline-sodic overburden at Syncrude's Mildred Lake Mine by Meiers et al. (2011) and was detected by Inverse Modelling (IM) by Huang et al. (2015b). Such observed temporal variability was assumed to be due to the changes in density and pore-size distribution as a result of freeze/thaw or wet/dry cycles, and vegetation establishment. Spatial variability would be expected to occur in reclamation covers as a result of material heterogeneity, cover construction/placement conditions, topography, or vegetation establishment. For example, Huang et al. (2016) were able to characterize the spatial variability of Ks using air-permeability testing of covers.

Quantifying spatial and temporal variability would be of value when the performance of reclaimed oil sands closure landscapes is being evaluated. However, the estimation of spatial and temporal variability (i.e. uncertainty in the model parameters) is not conventionally incorporated in the calibration of SVAT models or in the modelling of long-term cover performance.

Alam et al. (2017) undertook a preliminary evaluation of the uncertainty in the hydraulic properties of reclamation covers on the long-term water balance of oil sands reclamation covers. In that study, IM modelling was undertaken for four different reclamation covers (replicated in triplicate) over three monitoring years. The calibrated parameters showed that parameter uncertainty (variability) could be linked to both spatial and temporal variability but was dominated by spatial uncertainty.

The impact of vegetation development on AT was quantified using the leaf area index (LAI). Huang et al. (2017) found that LAI had the largest influence over the range of the water balance components, AT and NP.

Uncertainty in the soil hydraulic parameters also led to uncertainties in the range of LAI that was sustainable for a given cover design.

HYDRUS-1D has been used previously to characterize spatial and temporal variability in the soil hydraulic parameters (Harman et al. 2011; Qu et al. 2014; Alam et al. 2017). The objectives of this study were to use the IM modelling implemented in HYDRUS-1D to: (i) characterize uncertainty in the optimized parameters and LAI, and (ii) evaluate the impact that these sources of uncertainty have on the predicted long-term cover performance.

2 MATERIALS AND METHODS

2.1 Study Sites

The study used soil monitoring data and meteorological data from the Aurora Capping Study (ACS) located at Aurora North Mine in Alberta. Syncrude Canada Ltd. (SCL). The ACS is comprised of a series of 12 alternate cover designs, replicated in triplicate, placed over LOS. The primary purpose of different cover designs was to compare the performance of alternate materials and cover thicknesses in supporting vegetation and net percolation (OKC, 2017).

The layout of the 12 covers (replicated) are shown in Figure 1 and are designated as T#, where T denotes treatment cover and # denotes position from 1 to 12. Each of the replicated cover system designs is known as a "cell" with a total of 36 cells in the ACS. The 36 cells, representing 12 alternate cover designs randomly placed across a watershed as 36 one-hectare cells. The treatment covers were constructed with different reclamation materials including a variety of placement configurations and reclamation capping thicknesses, all over lean oil sand (LOS) substrate: i) an upper layer (coversoil) of either salvaged peat or upland leaf/folic/humic (LFH) plus a portion of the underlying A and possibly B horizons, and (ii) three types of sandy subsoil varying in their salvage depth. The various soil cover designs are summarized in Table 1. All of the subsoil materials have sandy textures (mean loamy sand texture) (Soil Classification Working Group, 1998). All of the 13 treatment covers (which includes two sub-categories of T12) were included in this study. Composition of the treatment cover materials and vegetation types can be found in Alam et al. (2017).

2.2 Field Monitoring Data

A climate monitoring station (Aurora Met) was established in 2012 to measure precipitation, air temperature, wind speed, net radiation, and relative humidity at the study site. In addition, each cell had a soil monitoring location where soil volumetric water content, temperature, and suction were measured at multiple depths within the treatment covers and the underlying LOS. Both meteorological and soil monitoring data for four consecutive growing seasons (2013-2016) were used to calibrate the physically-based SVAT model for each cell. This provided 155 optimized parameter values, which were interpreted to define spatial and temporal uncertainty in the hydraulic conductivity (Ks) and water retention curves (WRC). For the IM, the focus was on the three soil types such as peat (combining with LFH) overlying subsoil (combining one salvage depth, rather than discrete salvage depths) and LOS, as this has been typically used in oil sands reclamation cover design.

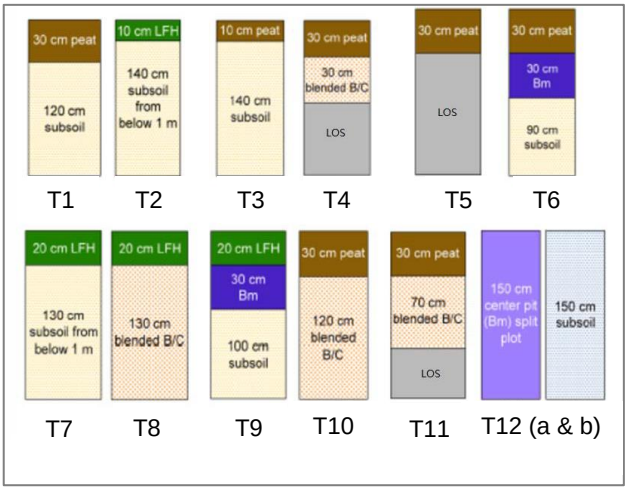

Figure 1. Soil cover design treatments (T) at ACS (O'Kane Consultants Inc., 2017). LOS underlies all treatments

2.3 Parameter Estimation Using Inverse Modelling

IM is a mathematical approach that estimates unknown causes (e.g. model parameters) using observed variables (e.g. water content or pressure heads) during a historical period by iteratively solving the governing equation (Hopmans et al. 2002).

HYDRUS-1D is a numerical solution to Richard's equation for water flow in unsaturated soils. Potential evapotranspiration (PET) is calculated from climatic conditions using the Penman-Monteith equation (Brutsaert, 1982). It is then apportioned into potential evaporation (PE) and potential transpiration (PT) based on a prescribed LAI value. The actual evaporation (AE) from the ground surface is calculated from the PE and some limiting water stress (i.e. suction) at the top of the soil profile. Whereas actual transpiration (AT) is calculated by distributing PT over a prescribed rooting zone where root water uptake is limited by water stress, as calculated by a root water uptake model (Feddes et al. 1974).

HYDRUS-1D embeds an IM method into the numerical solution of the Richard's equation. The IM method uses the Marquardt-Levenberg gradient-based approach (Simunek et al. 2013) in which the value of the five individual model parameters (i.e. θr, θs, α, n, Ks) are varied for each material until a combination is found that provides an optimal fit to the observed water content dynamics within the cover (Hopmans et al. 2002). How well these individual parameters are estimated determines the overall accuracy of parameter estimation. Details of IM used in HYDRUS-1D can be found in Simunek et al. (2013).

2.4 Discretization of Model Domain

The soil profile used in HYDRUS-1D had a maximum height of 2.5 m with a minimum of 1 m of LOS overlain by the various soil profiles (Table 1). The 2.5 m profile depth was chosen consistently for all the treatment covers so that parameter estimation was not a function of cover depth in addition to the cover material types. The spatial discretization used for all the model domains was 1-cm.

2.5 Vegetation and Root Distribution

Maximum LAI values for each treatment cover were estimated from photographs taken on site (OKC 2017) and varied from 0.2 at T5 to 1.5 at T2, T7, and T8. The distribution of LAI over the growing season was the same as that used by Huang et al. (2015): (a) a linear rise in the spring from zero to a maximum value, (b) maximum in the summer, and (c) linear decrease from the maximum value to zero in the fall.

The roots were assumed to be distributed within the cover soils using an exponential function of root mass with depth the maximum root mass at surface decreasing to zero at the base of the cover. The maximum root depths were measured to be 0.3 m at T5; 0.5 m at T1, T2, T3, T4, T6, T7, T8, T10, T11, T12a, T12b; and 1.0 m at T9 (Bockstette and Bockstette, 2016).

Table 1: Discretization of model domain for all treatment covers

Treatment	Depth (cm)		
	Peat or LFH	Subsoil**	LOS
T1	30	120	100
T2*	10	140	100
T3	10	140	100
T4	30	30	190
T5	30	-	220
T6	30	120	100
T7*	20	130	100
T8*	20	130	100
T9*	20	130	100
T10	30	120	100
T11	30	70	150
T12a	-	150	100
T12b	-	150	100

*Denotes treatment covers with LFH

**Subsoil material types vary with treatment, but are not described in the table

2.6 Estimation of Parameter Uncertainty

The IM modelling was undertaken using the monitored water content profiles at all the cells along with the site-specific meteorological data in each individual monitoring year. Since one cell of T5 was missing data in 2013, a total of 155 HYDRUS-1D models (12 treatments, 3 replicated cells, and 4 years of data) were calibrated by optimizing five soil hydraulic parameters for each soil type. The set of 155 optimized parameters for each soil type was used to characterize the uncertainty (both spatial and temporal) in estimating soil hydraulic parameters and the impact of this parameter uncertainty on the long-term cover performance.

2.7 Maximum Sustainable LAI

The key water balance components, AT and NP, are largely controlled by the selected LAI values (Huang et al. 2011b, 2017). Huang et al. (2011b) used literature-based relationships between above-ground net primary production (ANPP), LAI, and AT to constrain LAI_Max in the long-term simulations. Since the parameter uncertainty is expected to influence the long-term water balance (AT and NP) of the treatment covers, the ANPP-LAI-AT relationships are also expected to be influenced by the parameter uncertainty. Consequently, the uncertainty in the LAI_Max has an influence on long-term cover performance in combination with the parameter uncertainty.

2.8 Long-term Simulations with Parameter Uncertainty

The long-term cover performance was evaluated by simulating long-term climate records represented by 60 years of climate data from Fort McMurray Airport Weather Station. Uncertainty in the long-term cover performance was incorporated by simulating a hypothetical cover of 2.0-m (20-cm peat, 100-cm subsoil, and 80-cm LOS overburden) with optimized soil properties. Details of simulating hypothetical cover designs are available in Alam et al. (2017).

The impact of uncertainty in the parameters on the predicted long-term performance of a reclamation cover will be illustrated using a typical cover of peat overlying subsoil on LOS. As will be shown below, peat showed the highest uncertainty in the WRC and the LOS has the greatest uncertainty in Ks. As a consequence, three alternative WRCs (10^{th}, 50^{th}, and 90^{th} percentile) for peat and five alternative Ks (10^{th}, 25^{th}, 50^{th}, 75^{th} and 90^{th} percentile) for the LOS were identified from the distributions of optimized model parameters. These cases were run with eight different LAI_Max values of 0.5, 1.5, 2.0, 2.5, 3.0, 3.5, 4.0, and 4.5. These combinations provide 135 simulations of long-term water balance (Peat: 3 WRCs x 3 Ks; Subsoil: 1 WRC x 3 Ks; and LOS: 1 WRC x 5 Ks) for each LAI_Max scenario.

The use of a limited number of alternate parameter sets to define variability was intended to limit the simulation time periods. Further advancement of this approach using a more generalized Monte Carlo based selection process is ongoing.

3 RESULTS AND DISCUSSION

3.1 Performance of the SVAT Models

The IM modelling resulted in a mean absolute error (MAE) that varied from 0.005 to 0.086 and root mean square error (RMSE) varied from 0.006 to 0.131. Figure 2 shows the scatter plots for the calibrated SVAT models at the selected cells where the models seem to overestimate or underestimate the observed water contents. SVAT models for a few cells (e.g. T5, T9) exhibited lower R^2 values

(<0.6); however, their performance in terms of MAE (<0.08) and RMSE (<0.09) was reasonable. Overall, the 155 cell-specific models performed well in simulating the soil water contents.

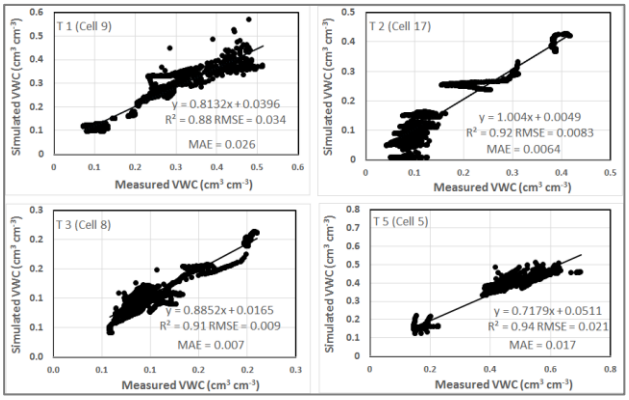

Figure 2. Comparison of the observed and simulated soil water contents for the HYDRUS-1D models for the selected cells

3.2 Uncertainty in the Optimized Parameters

3.2.1 Soil Hydraulic Parameters

Figure 3 shows the median of the five optimized parameters for three soil types with the inter-quartile box (i.e. 25% to 75%). The boxes were used to show the relative variability in the optimized parameters. The mean and SD values for the five parameters were used to calculate coefficient of variations (CV). These plots highlight that the peat had the highest variability in the WRC parameters while the LOS demonstrated the largest uncertainty in Ks.

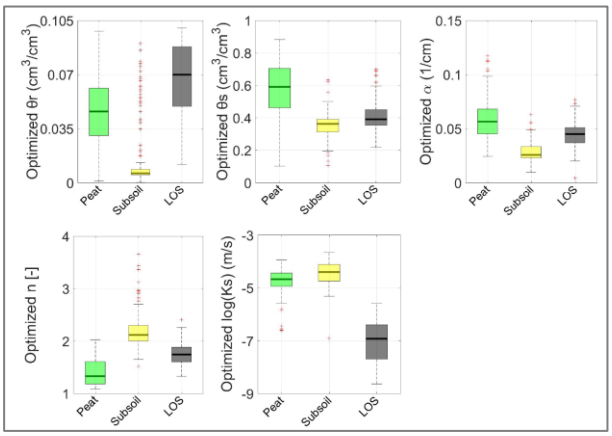

Figure 3. Distribution of the optimized hydraulic parameters for three soil layers of peat, subsoil and LOS overburden obtained from 155 calibrated models using inverse modelling. The box plots show: median, inter-quartile range, min, max, and outliers

Figure 4 shows the WRC for the three materials as represented by the mean optimized WRC as well as an envelope representing the 10th and 90th percentile values for the WRC. Among three material types, peat seems to show the largest uncertainty in estimating WRC. Higher uncertainties for the peat coversoil may be due to variable levels of organic matter decomposition and/or variable proportions of mineral inclusions.

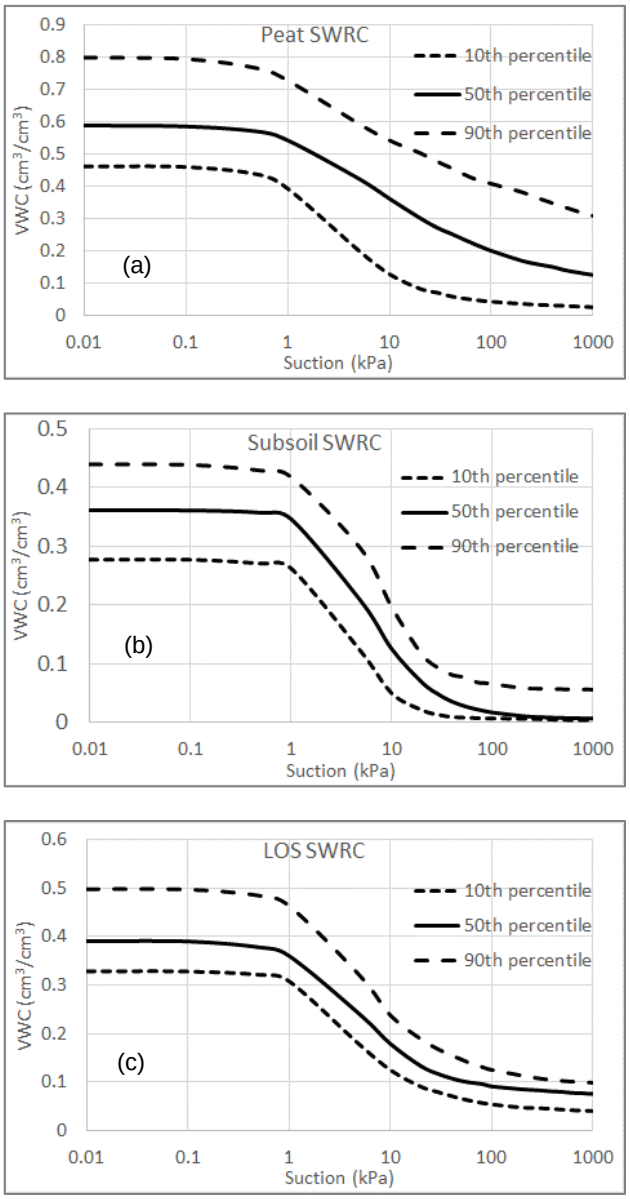

Figure 4. Uncertainty of estimated soil water retention curves (SWRC) for three material types (a) peat, (b) subsoil, and (c) LOS overburden, where VWC denotes volumetric water content

The optimized Ks values were compared to the Ks values obtained from direct field measurements (Huang et al.

2016). The field Ks values were measured using air permeameter (AP) and Guelph permeameter (GP) testing. Huang et al. (2016) showed that the Ks values from AP and GP testing produced very similar descriptions of variability although the mean Ks values were slightly offset, as might be expected. The distribution of Ks from the IM is compared to the field measured variability in Ks based on the cumulative frequency distributions (CFD). Figure 5 compares the CFD of the GP- and AP-measured Ks values with the optimized Ks values for three soil types. The measured and optimized Ks values have similar CFD shapes, Kolmogorov-Smirnov (KS) test confirmed similar CFD shapes for the peat and LOS soils. However, lower optimized Ks values for the subsoil have similar CFD as GP-measured Ks, while higher optimized Ks values have similar CFD as AP-measured Ks. Overall, the results suggest that the distribution of Ks obtained from IM do provide similar descriptions of spatial variability to that obtained from the direct testing.

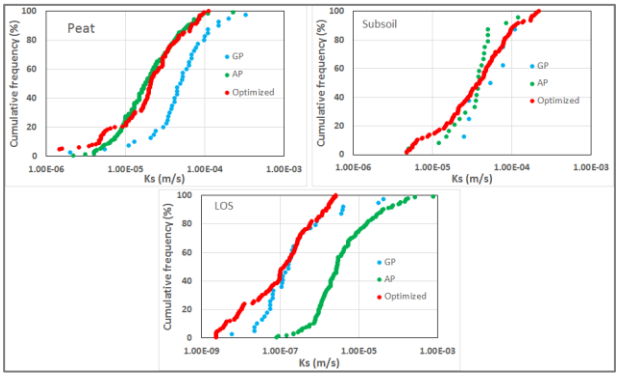

Figure 5. Comparison of the distributions of the measured field Ks using Guelph permeameter (GP) and Air permeameter (AP) with the optimized Ks values for peat, subsoil, and LOS

3.3 Uncertainty in Maximum Sustainable LAI

The uncertainty in the LAI_Max was evaluated by using the simulated annual AT values corresponding to the median, upper bound (90%), and lower bound (10%) of 135 realizations of the optimized parameters as shown in Figure 6. A line representing the annual AT required to support a particular LAI value is also plotted on this figure. This line represents the relationship between ANPP, AT, and LAI. The intersection points between the simulated and required AET lines designated as the LAI_Max. The range of LAI_Max values had a relatively narrow range from 2.6 to 3.4.

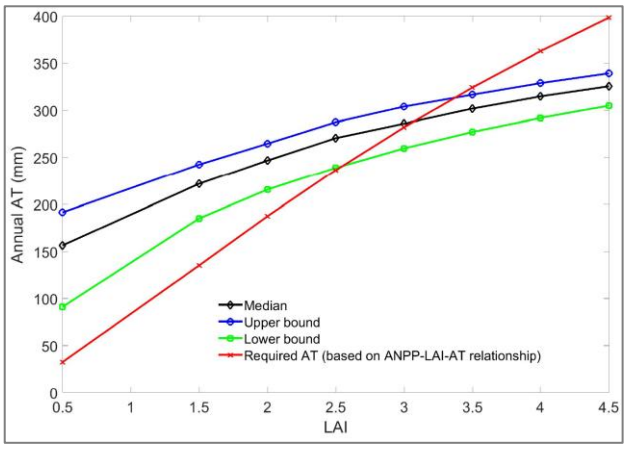

Figure 6. Lower, median, and upper limits of the LAI_Max values for D100 cover showing the uncertainty in the LAI values based on the simulated annual AT with the parameter uncertainty from the inverse modelling. D100 represents a hypothetical cover with a subsoil thickness of 1.0-m for ACS

3.4 Uncertainty in Water Balance Components

3.4.1 Actual Transpiration (AT)

The 10th and 90th percentile bounds for AT as obtained from the long-term simulation for each of the three LAI values are presented in Figure 7. These frequency distributions for annual AT values were obtained from the 135 simulations conducted using each LAI. The distribution highlights the impact of both climate variability (the climate data set) as well as parameter uncertainty. The impact of climate variability is represented by the range of AT values simulated while the relative vertical position of the three curves represents the impact of parameter uncertainty. The greatest range in AT between the upper and lower bound cases occurs between 20-35% of the non-exceedance probability. The maximum range of AT from the base case (median) based on these simulations is only +/- 14%.

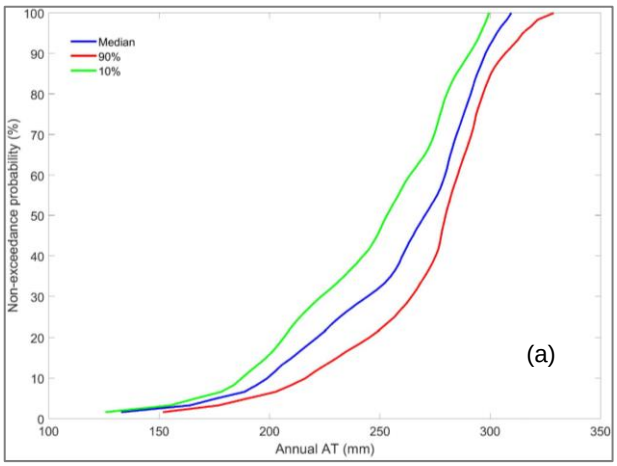

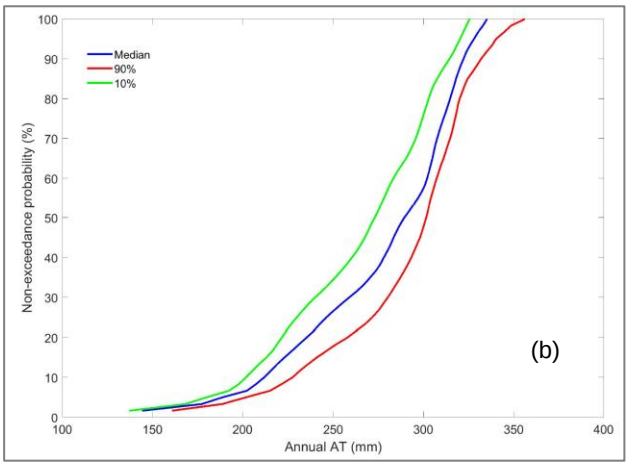

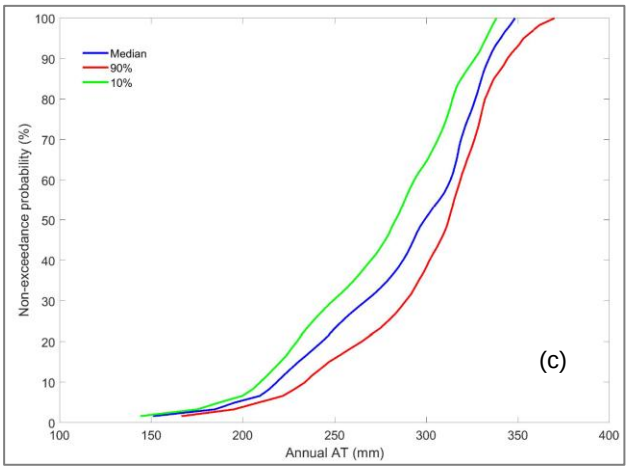

Figure 7. Frequency distribution and uncertainty of annual AT at the 10th, 50th, and 90th percentiles for D100 cover with the (a) lower (LAI = 2.6), (b) median (LAI = 3.1), and (c) upper bound (LAI = 3.4) of the LAI values

3.4.2 Net Percolation (NP)

The uncertainty in the simulated annual NP is shown in Figure 8 for three LAI values. The maximum uncertainty in estimating annual NP occurs approximately between 85-98% of the non-exceedance probability. The parameter uncertainty seems to result in higher uncertainty range in the frequency distributions of annual NP than those of annual AT. The maximum range of NP from the base case (median) based on these simulations would be +/- 212%.

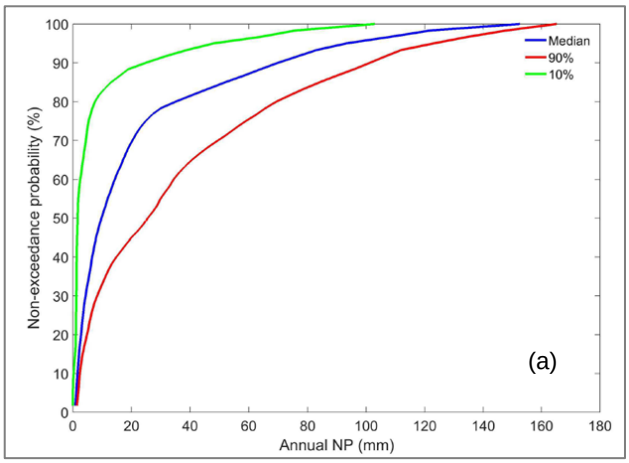

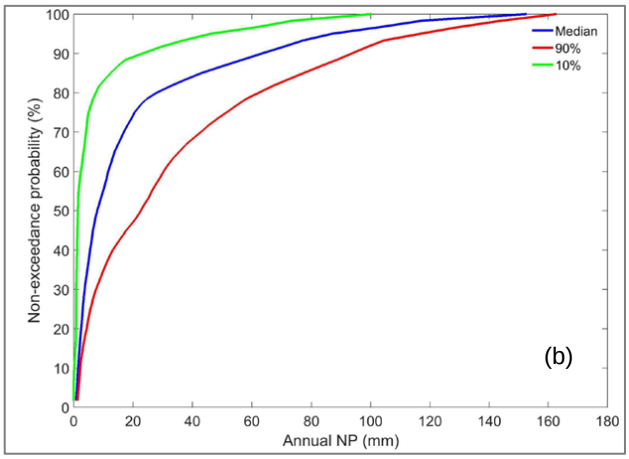

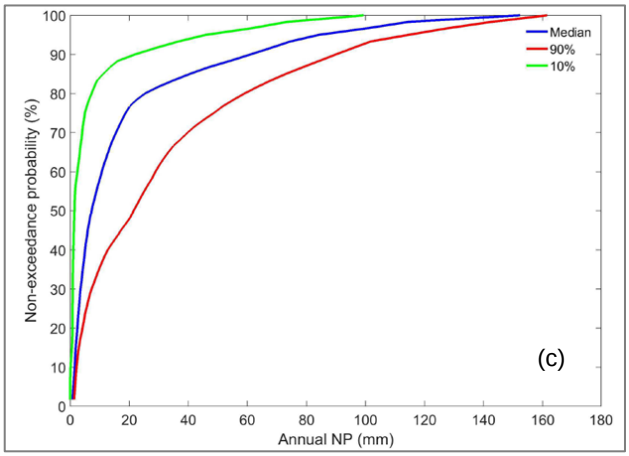

Figure 8. Frequency distribution and uncertainty of annual NP at the 10th, 50th, and 90th percentiles for D100 cover with the (a) lower (LAI = 2.6), (b) median (LAI = 3.1), and (c) upper bound (LAI = 3.4) of the LAI values

3.5 Uncertainty due to the choice of LAI

Figure 9 shows the frequency distributions for the mean annual AT and NP cases for the median, lower and upper LAI_Max values. Visual inspection of Figure 9(a) indicates

higher uncertainty in the annual AT than the range of uncertainty in annual NP in Figure 9(b). However, the simulated range of LAI values can result in maximum variations in the mean annual AT and mean annual NP of +/- 8% and 30%, respectively from the base LAI case (median). The maximum uncertainty in mean annual AT and NP occurs at non-exceedance probabilities of 50-100% and of 80-85%, respectively.

Figure 9 shows that the cumulative frequency distributions of annual NP are more skewed than those for the annual AT. The exceptionally skewed distributions of annual NP may be because wet years would produce very large NP, whereas AT in wet years would be constrained by PET.

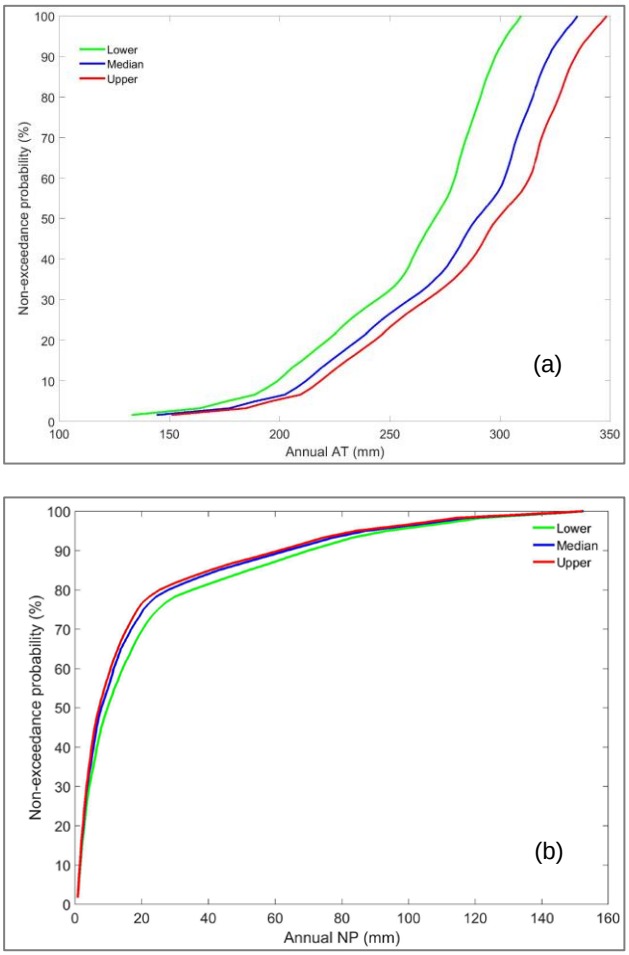

Figure 9. Frequency distribution and uncertainty of mean annual (a) AT and (b) NP during a 60-year water cycle for D100 cover with the lower, median, upper LAI values (LAI = 2.6, 3.1, and 3.4, respectively)

3.6 Sensitivity of Parameters in Simulating Water Balance

The simulated values of AT and NP from the long-term simulations were most sensitive to the selected LAI values. The simulated values of AT and NP were most sensitive to the Ks of the LOS. To illustrate this, the water balance simulations for a range of LOS Ks values were isolated and plotted in Figure 10. This figure highlights how the median annual AT decreases with increasing Ks while the median annual NP increases with the increasing Ks values.

Figure 10 also shows the ranges of uncertainty in the simulated annual AT and NP using five Ks values (0.07, 0.18, 1.04, 3.43, and 12.84 cm/day). At larger values of Ks there is more NP and less AT, as expected, however, with greater uncertainty in both of these parameters. As the value of Ks decreases both the values of AT and NP appear to become constant and with less uncertainty.

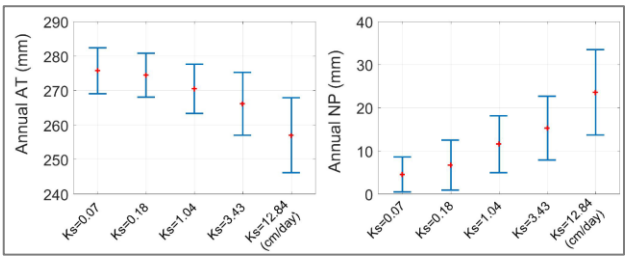

Figure 10. Uncertainty in the simulated water balance components (i.e. AT and NP) obtained for 135 combinations of soil hydraulic parameters, for instance, Ks for LOS overburden. Uncertainty of each water balance component is represented by the mean (red-cross) ± one standard deviation (blue vertical lines)

4 CONCLUSIONS

The inverse modelling of HYDRUS-1D was used to optimize five soil hydraulic parameters. The results from the IM modelling were then used in the simulation of long-term water balance for an illustrative cover. The results from this simulation were used to highlight the coupling that occurs between parameter uncertainty and the maximum sustainable LAI values as well as the combined impact of these sources of uncertainty on the predicted distributions of AT and NP.

The study revealed that peat coversoil had the highest uncertainty in the WRC compared to the subsoil and LOS. Among the three soil types and five soil hydraulic parameters, the Ks of the LOS had the largest uncertainty.

The results of the long-term simulation highlighted how both climate variability and parameter uncertainty will result in quite skewed variability in both AT and NP, particularly NP. The maximum difference (%) of the annual AT and NP from the base case (median) due to the climate and parameter variability can be 14% and 212%, respectively. The maximum difference (%) due to the LAI variability can be 8% and 30%, respectively. This highlights that in this case the parameter uncertainty exerts the greatest control over the long-term water balance variability.

Overall, the results of this study help to highlight that wide range of performance that can occur when parameter uncertainty is combined with climate variability. Further quantification of the contributions of spatial and temporal variability in the hydraulic properties of the cover soils will

improve our characterization and understanding of long-term cover performance beyond that which is possible with a single optimized parameter set and presumed value of LAI. Nevertheless, further research must examine the impact of a wide range of reclamation cover thicknesses as well.

5 ACKNOWLEDGEMENTS

The primary support from the National Science and Engineering Research Council of Canada (NSERC) and Syncrude Canada Ltd. (File No. 428588-11) is highly acknowledged. The authors thank Amy Heidman of O'Kane Consultants Inc. for providing an uninterrupted access to the Syncrude database.

6 REFERENCES

Alam, M.S., Barbour, S.L., Huang, M. and Doucette, L. 2017. An Evaluation of Parameter Uncertainty in the Calibration of a Soil-Vegetation-Atmosphere-Transfer (SVAT) model for a Reclamation Cover on LOS. *Proceedings of 70th Canadian Geotechnical Society Conference, GeoOttawa 2017*, Ottawa, Ontario, October 2-4.

Bockstette, J. and Bockstette, S. 2016. Personal data exchange, no paper and no report, University of Alberta.

Brutsaert, W. 1982. *Evaporation into Atmosphere: Theory, History, and Applications*. Dordrecht: D. Reidel Publishing Company, pp 302.

Feddes, R.A., Bresler, E. and Neuman, S.P. 1974. Field test of a modified numerical model for water uptake by root systems. *Water Resour. Res.*, 10, 1199–1206.

Harman, C.J., Rao, P.S.C., Basu, N.B., McGrath, G.S., Kumar, P. and Sivapalan, M. 2011. Climate, soil, and vegetation controls on the temporal variability of vadose zone transport. *Water Resour. Res.*, 47.

Hopmans, J.W., Simunek, J., Romano, N. and Durner, W. 2002. *Chapter 3.6.2: Inverse Methods*. In J.H. Dane G.C. Topp Methods Soil Anal. Part 4. Phys. methods. SSSA B. Ser. 5. SSSA, Madison, WI.

Huang, M., Elshorbagy, A., Barbour, S.L., Zettl, J. and Si, B.C. 2011a. System dynamics modeling of infiltration and drainage in layered coarse soil. *Can J Soil Sci*, 91(2): 185–197. doi.org/10.4141/cjss10009

Huang, M., Barbour, S.L., Elshorbagy, A., Zettl, J. and Si B.C. 2011b. Water availability and forest growth in coarse-textured soils. *Can J Soil Sci*, 91(2): 199–210. doi.org/10.4141/cjss10012

Huang, M., Barbour, S.L., Elshorbagy, A., Zettl, J.D. and Si B.C. 2011c. Infiltration and drainage processes in multi-layered coarse soils. *Can J Soil Sci*, 91(2): 169–183. doi.org/10.4141/cjss09118

Huang, M., Barbour, S.L. and Carey, S.K. 2015a. The impact of reclamation cover depth on the performance of reclaimed shale overburden at an oil sands mine in Northern Alberta, Canada. *Hydrol Process*, 29(12): 2840–2854. doi.org/10.1002/hyp.10229

Huang, M., Rodger, H. and Barbour, S.L. 2015b. An evaluation of air permeability measurements to characterize the saturated hydraulic conductivity of soil reclamation covers. *Can. J. Soil Sci.* 95: 15–26.

Huang, M., Zettl, J.D., Barbour, S.L. and Pratt, D. 2016. Characterizing the spatial variability of the hydraulic conductivity of reclamation soils using air permeability. *Geoderma*, 262: 285–293.

Huang, M., Alam, S., Barbour, L. and Si, B. 2017. Numerical modelling of the impact of cover thickness on the long-term water balance of reclamation soil covers over lean oil sands overburden. *Report prepared for Syncrude Canada Ltd.*

Keshta, N., Elshorbagy, A. and Carey, S. 2009. A generic system dynamics model for simulating and evaluating the hydrological performance of reconstructed watersheds. *Hydrol Earth Syst Sci*, 13(6): 865–881. doi.org/10.5194/hess-13-865-2009

Meiers G., Barbour S.L., Qualizza C. and Dobchuk, B. 2011. Evolution of the hydraulic conductivity of reclamation covers over sodic/saline mining overburden. *J. Geotech. Geoenv. Engrg*, 137(1): 968–976.

O'Kane Consultants Inc. (OKC). 2017. Aurora Soil Capping Study Five Year Performance Monitoring Report November 2012 to September 2017. *Report No. 690/141--001.*

Price, J.S., McLaren, R.G. and Rudolph, D.L. 2010. Landscape restoration after oil sands mining: conceptual design and hydrological modelling for fen reconstruction. *Int J Mining Reclam Environ*, 24(2): 109–123. doi.org/10.1080/17480930902955724

Qu, W., Bogena, H.R., Huisman, J.A., Martinez, G. Pachepsky, Y.A. and Vereecken, H. 2014: Effects of Soil Hydraulic Properties on the Spatial Variability of Soil Water Content: Evidence from Sensor Network Data and Inverse Modeling. *Vadose Zo. J.*, 13.

Qualizza, C., Chapman, D., Barbour, S.L. and Purdy, B. 2004. Reclamation research at Syncrude Canada's mining operation in Alberta's Athabasca oil sands region. *In: Proceedings of the 16th International Conference on Ecological Restoration SER2004*, Victoria, BC 24-26 August.

Simunek, J., Šejna, M., Saito, H., Sakai, M. and van Genuchten, M.T. 2013. The HYDRUS-1D Software Package for Simulating the One-Dimensional Movement of Water, Heat, and Multiple Solutes in Variably-Saturated Media. University of California, Riverside, CA.

Soil Classification Working Group. 1998. Canadian System of Soil Classification. NRC Research Press, Research Branch, Agriculture and Agri-Food Canada. Ottawa, Canada. Publication 1646, 3rd edition.